2
Physicochemical Approaches to Studying Plant Growth Promoting Rhizobacteria

Alexander A. Kamnev

2.1
Introduction

Within the last few decades, the application of instrumental techniques in scientific research related to life sciences and biotechnology has been rapidly expanding. This trend largely concerns biochemistry and biophysics, thus reflecting the interpenetration and interrelationship between different fields of natural sciences in studying biological objects [1]. Albeit to a lesser degree, the use of physicochemical techniques is increasingly being put into practice in microbiology. The possibility of obtaining reliable, selective and sometimes unique information about sophisticated biological systems under study at different levels of their organization (e.g. organism, tissue, cell, cellular supramolecular structures, biomacromolecules, low-molecular-weight metabolic products, etc.) and functioning is an attractive feature of modern instrumental techniques. In addition, some techniques are nondestructive and/or provide information on intact biological matter with a minimum of sample preparation, which most closely reflects its natural state. Moreover, the bioanalytical information obtained by a combination of independent instrumental techniques may be of significant advantage, especially when comparing data on overall cellular metabolic changes (e.g. as cellular responses to some environmental factors) with analyses for microelements (e.g. trace metal uptake) and/or their chemical forms (speciation analysis).

The scientific literature of recent decades provides evidence that the field of plant growth promoting rhizobacteria (PGPR) and their interactions with host plants is highly promising for possible wide-scale applications in returning to environmentally friendly and sustainable agriculture. However, there are still a great number of problems related to the basic mechanisms of the underlying biological and chemical processes that occur both in the rhizosphere and *in vivo* (in plants and PGPR), which require systematic research at the molecular level using modern techniques.

In this chapter, some recent examples are discussed which illustrate the use of various physicochemical and spectroscopic approaches, involving a range of

Plant-Bacteria Interactions. Strategies and Techniques to Promote Plant Growth
Edited by Iqbal Ahmad, John Pichtel, and Shamsul Hayat

ISBN: 978-3-527-31901-5

instrumental techniques, aimed at obtaining structural and compositional data related to PGPR, their cellular biopolymers and secondary metabolites. Particular attention is paid to the behavior of PGPR, using the example of the widely studied ubiquitous diazotrophic plant-associated rhizobacterium *Azospirillum brasilense* [2], and the effect of various environmental factors upon it.

2.2 Application of Vibrational Spectroscopy to Studying Whole Bacterial Cells

2.2.1 Methodological Background

Cellular metabolic processes, including their alterations induced by various environmental factors, largely result in qualitative and/or quantitative compositional changes in microbial cells. Knowledge of such changes is of importance both for basic studies (e.g. on the molecular mechanisms of microbial responses to environmental stresses) and for applied research (e.g. monitoring of fermentation processes, in agricultural microbiology and biotechnology, clinical microbiology and diagnostics). In addition to 'wet' chemical analysis and biochemical methods, such changes can be controlled in microbial biomass or even in single cells using various modifications of vibrational (Fourier transform infrared [FTIR], FT-Raman) spectroscopy [3–7]. In recent years, microbiological applications of these techniques have been developed to the level of convenient and sensitive tools for monitoring both macroscopic changes in the cellular composition and fine structural rearrangements of particular cellular constituents (see, e.g. [6–10] and references therein).

An absorption spectrum in the case of conventional FTIR spectroscopy [3,4,6,10], as well as a FT-Raman scattering spectrum [3,5,7], of a sample of biomass comprising, for instance, whole bacterial cells presents a complicated summarized image. Contributions to such a spectrum are made by all the major cellular constituents (or, more exactly, their functional groups with their characteristic vibration frequencies, including also the effects of all possible molecular, atomic and/or ionic interactions). In the first instance, these are proteins and glycoproteins, polysaccharides, lipids and other biomacromolecules. As a consequence, a spectrum reflects the overall chemical composition of the cell biomass, which in certain cases can be used for identification and classification of microorganisms [3,6,9] based on differences in qualitative and/or quantitative composition of their cells.

2.2.2 Vibrational Spectroscopic Studies of *A. brasilense* Cells

2.2.2.1 Effects of Heavy Metal Stress on *A. brasilense* Metabolism

Bacteria of the genus *Azospirillum* have been well documented to demonstrate relatively high tolerance to moderate heavy metal stress [2,11,12]. This feature

may well be of advantage for agricultural applications of these PGPR in metal-contaminated environments [2,11] or for enhancing phytoremediation [13–17], in particular, based on using heavy metal accumulating plants. In the presence of submillimolar concentrations of conventionally toxic metals which do not significantly suppress growth of azospirillum [10,12], *A. brasilense* was found to take up and accumulate noticeable amounts of heavy metals (e.g. vanadium, cobalt, nickel, copper, zinc and lead), which were also shown to influence the uptake of essential elements (magnesium, calcium, manganese and iron) [18]. In particular, the uptake of iron (present in the medium as Fe^{2+}) was drastically reduced (by about 1 order of magnitude) in the presence of 0.2 mM Co^{2+}, Ni^{2+} or vanadium(IV) (VO^{2+}) salts, probably reflecting their competitive binding to iron chelators and transporters to the cell.

One of the conspicuous effects was an increased accumulation of the four essential cations (about two- to fivefold) in the presence of 0.2 mM copper(II) in the culture medium (while Cu was also accumulated by the bacterium up to 2 mg g^{-1} of dry cell biomass) [18]. This effect induced certain alterations in the FTIR spectra of both whole cells [19] and cell membranes (note that in *A. brasilense* membranes, in contrast to whole cells, only the Mg^{2+} content was increased approximately sixfold in the presence of Cu^{2+}) [20] as well as in electrophysical properties of the bacterial cell surface [21]. It has to be noted that the aforementioned experiments on azospirillum [18–20] were performed, besides being under moderate heavy metal stress conditions, in an NH_4^+-free phosphate–malate medium corresponding to a high C : N ratio. This kind of nutritional stress (i.e. bound nitrogen deficiency) is known to induce accumulation of a reserve storage material, poly-3-hydroxybutyrate (PHB), along with other polyhydroxyalkanoates (PHA), playing a role in stress tolerance in many bacteria, including *A. brasilense* [22,23]. Accordingly, signs of polyester accumulation were also noticeable in FTIR spectra of *A. brasilense* cells grown under nitrogen deficiency [19].

A subsequent FT-Raman spectroscopic study of whole cells of *A. brasilense* (non-endophyte strain Sp7), grown in a rich ammonium-supplemented medium in the presence of 0.2 mM Co^{2+}, Cu^{2+} or Zn^{2+} salts, suggested that some metabolic changes occur induced by the heavy metals [7]. In particular, besides some subtle changes in cellular lipid-containing constituents (to which FT-Raman spectroscopy is highly sensitive [3,5,7]), accumulation of some polymeric material could be proposed. Since the induction of PHA or PHB biosynthesis by heavy-metal stress alone, without a nutritional stress, had not been earlier described in bacteria [24] (for a recent review see [23] and references therein), an attempt was made to use FTIR spectroscopy which is more sensitive to polyester compounds [3,4,6,10].

2.2.2.2 Differences in Heavy Metal Induced Metabolic Responses in Epiphytic and Endophytic *A. brasilense* Strains

Whole cells of *A. brasilense* (non-endophyte strain Sp7) grown in a standard medium (control) and in the presence of several heavy metals (0.2 mM Co^{2+}, Cu^{2+} or Zn^{2+}) were analyzed using FTIR spectroscopy [24]. Striking differences were noticeable in the FTIR absorption profiles between the control cells (Figure 2.1a) and cells grown

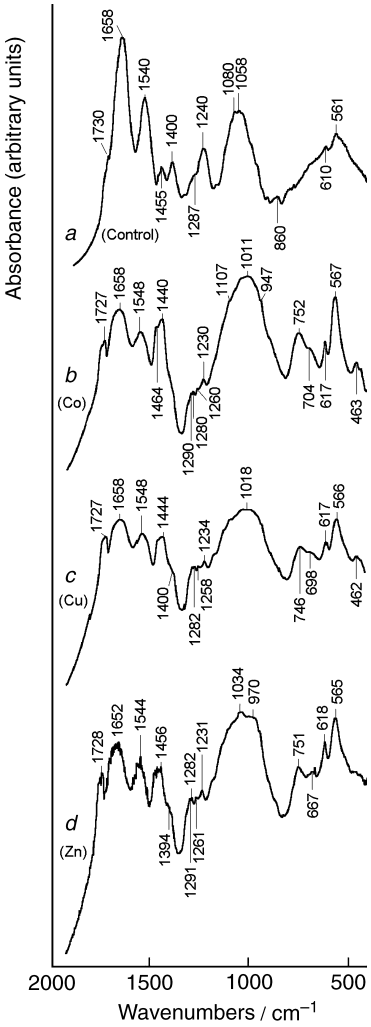

Figure 2.1 Infrared spectra of dried biomass of *A. brasilense* (non-endophytic strain Sp7) grown (a) in a standard phosphate–malate medium (control) and in the same medium in the presence of 0.2 mM Co^{2+} (b), Cu^{2+} (c) or Zn^{2+} (d) [10,24].

under moderate heavy metal stress (Figure 2.1b–d). The most prominent feature of the metal-stressed cells is the appearance of a relatively strong and well-resolved band at about 1727 cm^{-1} (Figure 2.1b–d) featuring polyester ν(C=O) vibrations. On the contrary, in the control cells where the amide I and amide II bands of cellular proteins (at about 1650 and 1540 cm^{-1}, respectively) dominate (Figure 2.1a), there is only a weak shoulder at about 1730 cm^{-1}. Together with an increased FTIR absorption in the regions of methylene ($-CH_2-$) bending vibrations (at 1460–1440 cm^{-1}),

as well as C−O−C and C−C−O vibrations (at 1150–1000 cm^{-1}) and CH_2 rocking vibrations (at about 750 cm^{-1}) observed in metal-stressed cells (Figure 2.1b–d), these spectroscopic changes provide unequivocal evidence for the accumulation of polyester compounds in cells of strain Sp7 as a response to metal stress.

As mentioned above, PHB has been documented to accumulate in cells of azospirilla under unfavorable conditions, playing a role in bacterial tolerance to several kinds of environmental stresses [22,23] and providing a mechanism that facilitates bacterial establishment, proliferation, survival and competition in the rhizosphere [25]. However, under normal conditions, particularly in nitrogen-supplemented media, its biosynthesis is usually suppressed [22]. Thus, the induction of biosynthesis and accumulation of PHB (and possibly other PHAs) under normal nutritional conditions by heavy metals is a novel feature for bacteria (which was for the first time documented for *A. brasilense* Sp7 [24]), which is in line with the overall strategy of bacterial responses to stresses. It has to be noted that, although cellular lipids can give similar FTIR spectroscopic signs, an accumulation of additional lipids is not physiologically appropriate for azospirilla [2,26].

Within the *A. brasilense* species, there is a unique possibility to compare the behavior of epiphytic strains (which colonize the rhizoplane only) and endophytic ones [27]. In view of that, it is of interest to compare the response of the latter to heavy metals. A comparison of FTIR spectroscopic images of another *A. brasilense* strain, Sp245 (which, in contrast to strain Sp7, is a facultative endophyte [27,28]), grown under similar conditions in the standard medium and in the presence of each of the above three cations (0.2 mM), shows no major differences between them (Figure 2.2a–d). In all four samples, there is a weak shoulder at about 1730 cm^{-1} (ester ν(C=O) band), but in metal-stressed cells there occurs virtually no accumulation of PHA that was found under similar conditions in strain Sp7 (Figure 2.1). Moreover, the position of the representative $\nu_{as}(PO_2^-)$ band of cellular phosphate moieties in strain Sp245 was constant within the relatively narrow region 1237–1240 cm^{-1}, thus confirming the relative stability of the state of these functional groups both in the control group of cells and those under metal stress (whereas in metal-stressed cells of strain Sp7, this band was found at lower frequencies, 1230–1234 cm^{-1}; Figure 2.1b–d). This finding is remarkable, especially considering the comparable uptake level of each of the cations in the bacterial cells of the two strains (0.12 and 0.13 mg Co, 0.48 and 0.44 mg Cu, 4.2 and 2.1 mg Zn per gram of dry cells for strain Sp7 and Sp245, respectively) [10].

Thus, the response of the endophytic *A. brasilense* strain Sp245 to a moderate heavy metal stress was found to be much less pronounced than that of the non-endophyte strain Sp7. These conspicuous dissimilarities in their behavior may be related to different adaptation abilities of the strains under stress conditions owing to their different ecological status and, correspondingly, different ecological niches which they can occupy in the rhizosphere. In the non-endophytic strain, PHB/PHA accumulation may be a specific flexible adaptation strategy related to the localization of the bacteria in the rhizosphere and on the rhizoplane, i.e. always in direct contact with rhizospheric soil components, in contrast to the endophyte which is somewhat more 'protected' by plant tissues [29]. This corresponds to the documented capability

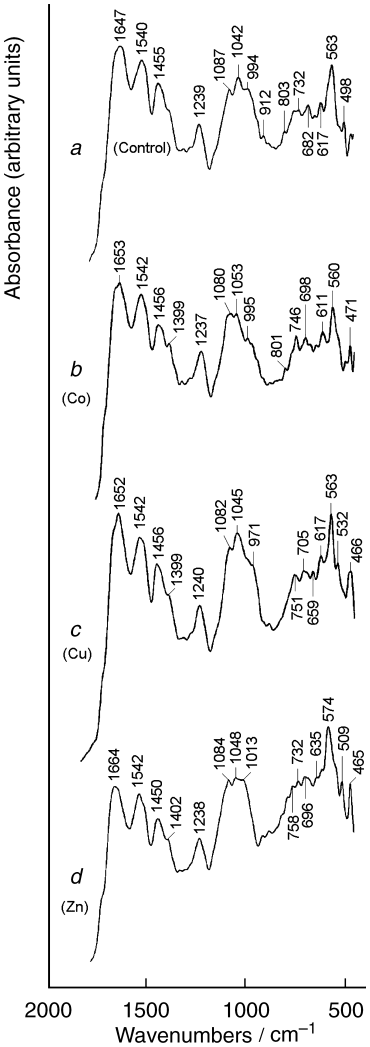

Figure 2.2 Infrared spectra of dried biomass of *A. brasilense* (facultatively endophytic strain Sp245) grown (a) in a standard phosphate–malate medium (control) and in the same medium in the presence of 0.2 mM Co^{2+} (b), Cu^{2+} (c) or Zn^{2+} (d) [10].

of strain Sp7 to outcompete other co-inoculated strains [27], as well as to a lower sensitivity of strain Sp7, as compared to strain Sp245, to copper ions, including a less pronounced copper-induced decrease in auxin production [12,30].

As noted above, the amount of cobalt accumulated by strain Sp7 (up to about 0.01% wt/wt dry biomass) induces a significant metabolic response in the bacterium, comparable to that of about fourfold higher amount of copper or about 36-fold

higher amount of zinc (cf. Figure 2.1a–d). Moreover, such amounts of metal complexes per se cannot give any clearly noticeable FTIR absorption related to their intrinsic functional groups. Thus, in strain Sp7 such a moderate heavy metal stress evidently induces noticeable metabolic transformations that are revealed in their FTIR spectra as macroscopic compositional changes. In its turn, this suggests direct participation of the cations, which are taken up by the bacterial cells from the medium, in cellular processes as a result of their assimilation. However, for strain Sp245, despite the levels of metal uptake comparable with those for strain Sp7, this is not obvious, considering the lack of noticeable compositional changes revealed by FTIR spectroscopy (Figure 2.2).

In order to validate the direct involvement of metal cations in cellular metabolic processes in strain Sp245, the chemical state of accumulated trace metal species must be monitored in live cells for various periods of time. Some examples of microbiological applications of a technique, which allows such monitoring to be made specifically for cobalt ions, are discussed below.

2.3
Application of Nuclear γ-Resonance Spectroscopy to Studying Whole Bacterial Cells

2.3.1
Methodological Background

Nuclear γ-resonance (Mössbauer) spectroscopy, based on recoil-free absorption (or emission) of γ-quanta by specific nuclei (the stable ^{57}Fe isotope having been so far most widely used), is a widely applicable powerful and informative technique, providing a wealth of information on the chemical state and coordination structure of the cation influenced by its microenvironment. The ^{57}Fe absorption variant of Mössbauer spectroscopy has been extensively used in a variety of fields including biological sciences, largely for studying Fe-containing proteins or for monitoring the state of iron species in biological samples (for recent reviews see, e.g. [31,32] and references therein).

The emission variant of Mössbauer spectroscopy (EMS), with the radioactive ^{57}Co isotope as the most widely used nuclide, is several orders of magnitude more sensitive than its ^{57}Fe absorption counterpart. However, despite the incomparably higher sensitivity of the former, applications of EMS in biological fields have so far been fragmentary and sparse, primarily owing to specific difficulties related to the necessity of using radioactive ^{57}Co in samples under study [33]. Note that radioactive decay of ^{57}Co (which has a half-life of 9 months), proceeding via electron capture by its nucleus, results in the formation of ^{57}Fe in virtually the same coordination microenvironment as the parent ^{57}Co cation. The decay process is accompanied by emission of a γ-quantum, as well as by some physical and chemical aftereffects which, in particular, often lead to the partial formation of stabilized daughter ^{57}Fe cations in oxidation states other than the parent ^{57}Co ones [34,35]. This effect, although inevitably complicating the emission spectra, can provide valuable

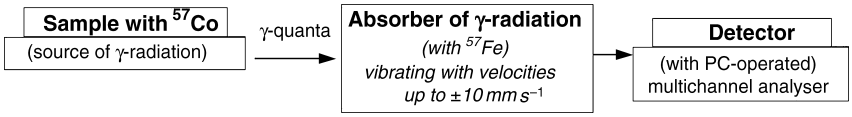

Figure 2.3 Scheme of experimental setup for measuring emission Mössbauer spectra [33].

additional information, e.g. on the electron-acceptor properties of the proximal coordination environment of the metal under study [35].

The recoil-free emission (as well as absorption) of γ-radiation (i.e. the Mössbauer effect) is observed in solids only, where the recoil energy can dissipate within the solid matrix. Therefore, solutions or liquids are usually studied when they are rapidly frozen [34]. Rapid freezing (e.g. by immersing small drops or pieces of a sample in liquid nitrogen) often allows crystallization of the liquid (solvent) to be avoided, so that the structure of the resulting glassy solid matrix represents that of the solution. Moreover, upon freezing, all the ongoing biochemical (metabolic) processes in live cells, tissues or other biological samples cease at a certain point. Thus, for live bacterial cells that have been in contact with $^{57}Co^{2+}$ traces, freezing of suspension aliquots, taken after different periods of time, allows both the initial rapid binding of the metal cation by cell-surface biopolymers and its possible further metabolic transformations to be monitored.

A scheme of the experimental setup for measuring emission Mössbauer spectra is shown in Figure 2.3 [33]. The ^{57}Co-containing sample (which in EMS is the source of γ-radiation) can be kept in a cryostat (e.g. in liquid nitrogen at $T \approx 80$ K) with a window for the γ-ray beam, whereas the ^{57}Fe-containing standard absorber vibrates along the axis "source–absorber" at a constant acceleration value (with its sign changing periodically from $+a$ to $-a$, so that the range of velocities is usually up to ± 10 mm s^{-1} relative to the sample), thus modifying the γ-quanta energy scale as a function of velocity according to the Doppler effect. EMS measurements are commonly performed using a conventional constant-acceleration Mössbauer spectrometer calibrated using a standard (e.g. α-Fe foil) and combined with a PC-operated multichannel analyzer, where each channel represents a point with a specified fixed velocity. Standard PC-based statistical analysis consists of fitting the experimental data obtained to a sum of Lorentzian-shaped lines using a least squares minimization procedure. The Mössbauer parameters calculated from the experimental data are the isomer shift (IS; relative to α-Fe), quadrupole splitting (QS), linewidth (i.e. experimentally obtained full width at half maximum, FWHM), and relative areas of subspectra (S_r) [32–34].

2.3.2
Emission Mössbauer Spectroscopic Studies of Cobalt(II) Binding and Transformations in *A. brasilense* Cells

In order to check whether in *A. brasilense* Sp245 cobalt(II) ions are merely bound by the cell surface in a purely chemical process or cobalt(II) is assimilated and

somehow involved in metabolic processes, time-resolved EMS measurements could be performed using traces of $^{57}Co^{2+}$ salt. For strain Sp245, which had previously been shown to be tolerant to submillimolar concentrations of heavy metals, including cobalt(II) [10,12,18,19,30], EMS studies were, for the first time, performed on freeze-dried bacterial samples (rapidly frozen after 2–60 min of contact with $^{57}Co^{2+}$ salt and measured at $T = 80$ K) [36]. The following experiments, with the same strain were performed using suspensions of live bacteria rapidly frozen after the same periods of time (2–60 min) of contact with [^{57}Co]-cobalt(II), and EMS spectra were measured for frozen samples without drying, which more closely represented the state of cobalt in the live cells [37]. Nevertheless, comparing the data for freeze-dried bacteria [36] and for those measured in frozen aqueous suspensions [37] showed that their corresponding Mössbauer parameters were very close (both for 2 and 60 min contact with $^{57}Co^{II}$, whereas there were significant differences in the parameters between the two periods).

Typical EMS spectra of a rapidly frozen cell suspension and cell-free supernatant liquid shown in Figure 2.4 also clearly indicate differences between them. Note that two chemical forms referring to cobalt(II) were found in all samples. The [^{57}Co]-cobalt(II) forms are represented by quadrupole doublets with larger QS values (note that the third doublet with smaller IS and QS values corresponds to the aliovalent daughter [^{57}Fe]-ferric form resulting from aftereffects [33,37]). Multiple forms of cobalt(II) found in the spectra are related to the availability of different functional groups (with possibly different donor atoms) as ligands at the cell surface of *Azospirillum* [2].

In Figure 2.5, the Mössbauer parameters (IS and QS represented by points with their confidence intervals) are plotted for different cobalt(II) forms in each sample for various periods of contact (2 and 60 min) of the live bacteria with $^{57}Co^{II}$, as well as for dead bacterial cells (treated at 95 °C in the medium for 1 h in a water bath) and for the cell-free supernatant liquid [33]. Thus, each point with its confidence intervals (a rectangle) in Figure 2.5 corresponds to a separate $^{57}Co^{II}$ form with its characteristic microenvironment. Note that the parameters for both forms of [^{57}Co]-cobalt(II) show statistically significant difference for different periods of contact (2 and 60 min) of live bacteria with the metal. This shows that cobalt(II) is first rapidly absorbed by live *A. brasilense* cells in a merely chemical process, but then undergoes metabolic transformation within an hour. This finding confirms its direct involvement in bacterial metabolism, although in strain Sp245 (in contrast to strain Sp7) cobalt(II) assimilation is not accompanied by PHB accumulation (see above).

Interestingly, the parameters of the two forms of [^{57}Co]-cobalt(II) for live bacteria after 2 min, on the one hand, and for dead bacteria, on the other hand are rather close (essentially overlapping; Figure 2.5). This finding indicates that the mechanism of primary rapid Co^{2+} absorption by live cells is similar to the purely chemical binding process occurring at the surface of dead (thermally killed) cells, and is virtually unaffected by such hydrothermal treatment. Note also that the parameters for the cell-free supernatant liquid (from which the bacterial cells were removed by centrifugation) are clearly different from those for all other samples (Figure 2.5).

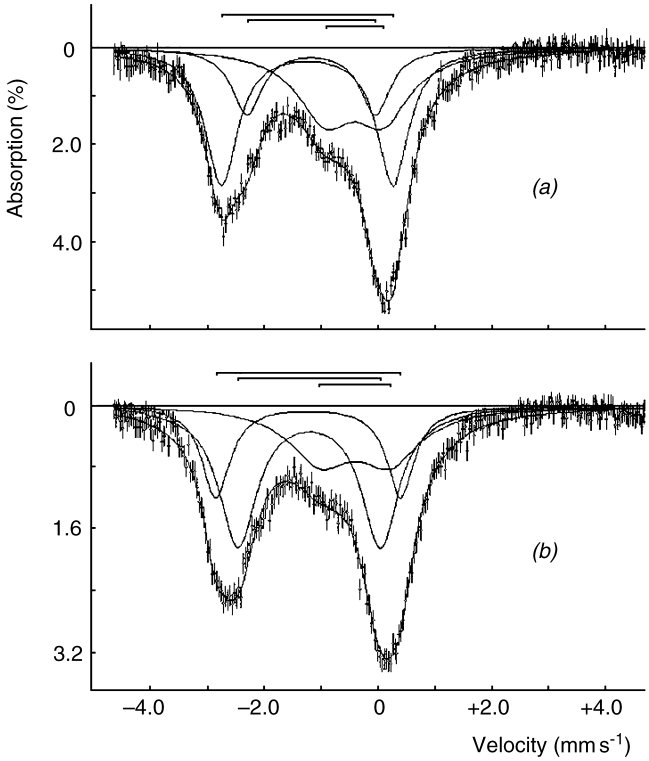

Figure 2.4 Typical emission Mössbauer spectra of (a) aqueous suspension of live cells of *A. brasilense* Sp245 in the culture medium (frozen 2 min after contact with $^{57}Co^{II}$ traces) and (b) the cell-free supernatant liquid rapidly frozen in liquid nitrogen (spectra collected at $T = 80$ K; velocity scale calibrated relative to α-Fe; intensities converted to the absorption convention) [37]. For each spectrum, the relevant subspectra (quadrupole doublets) are shown which contributed to the resulting spectrum (solid-line envelope) obtained by computer fitting to the experimental data (points with vertical error bars). The positions of the spectral components (quadrupole doublets) are indicated by horizontal square brackets above the zero lines.

It should be mentioned that primary binding of heavy metals by the cell surface in Gram-negative bacteria is mediated by capsular polysaccharide (PS, particularly carboxylated acidic PS), lipopolysaccharide (LPS, including phosphate LPS moieties), and proteinaceous materials [8,10,37]. In *A. brasilense*, these biopolymers and their covalently bound complexes characteristic of the cell surface [2] are believed to be involved in contact interactions with plant roots and in bacterial cell aggregation [2,25]. Thus, their interactions with metal ions in metal-contaminated soil can interfere with the processes of molecular plant–bacterial interactions, which must be investigated in detail. It has to be noted also that the above-described microbiological EMS studies can be applied for revealing possible biotransformations of environmentally significant ^{60}Co radionuclide traces that can result in its microbially mediated migration in soils and aquifers [10,12,38].

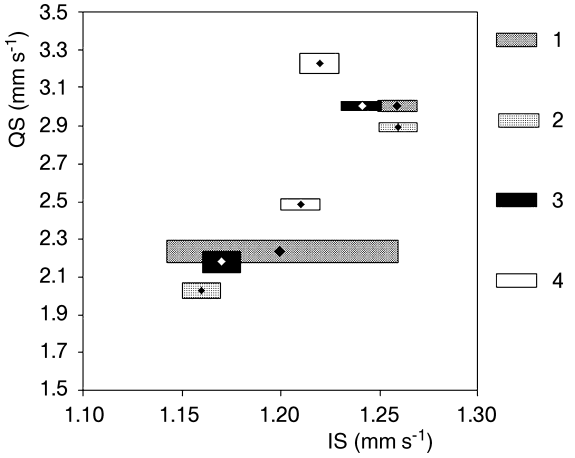

Figure 2.5 Comparison of Mössbauer parameters – isomer shift (IS, mm s^{-1}; relative to α-Fe) and quadrupole splitting (QS, mm s^{-1}) – calculated for the subspectra corresponding to different forms of [^{57}Co]-cobalt(II) in aqueous suspension of live cells of *A. brasilense* Sp245 rapidly frozen after (1) 2 min and (2) 60 min of contact with $^{57}Co^{II}$, (3) dead cells (hydrothermally treated at 95 °C for 1 h), as well as in cell-free supernatant liquid (4) (all spectra measured at $T = 80$ K) [33].

2.4
Structural Studies of Glutamine Synthetase (GS) from *A. brasilense*

2.4.1
General Characterization of the Enzyme

GS (EC 6.3.1.2), which catalyzes the ATP- and metal-ion-dependent synthesis of L-glutamine from L-glutamic acid and NH_4^+, is a key enzyme of nitrogen metabolism in many organisms from mammals to bacteria [39]. In diazotrophic PGPR, which contribute in part to the overall soil fertility and plant–bacterial interactions by fixing atmospheric nitrogen, basic knowledge of the structural and functional aspects of this enzyme at the molecular level is of special importance.

Regulation of activity and biosynthesis of bacterial GSs is very complex and has so far been investigated in detail for enteric bacteria only [39–41]. Glutamine synthetase activity in many bacteria, including *A. brasilense*, is modulated by reversible adenylylation of its subunits in response to the cellular nitrogen status. The enzyme is maintained in a top-active unadenylylated or slightly adenylylated form under nitrogen-limiting conditions, while its adenylylation state (ranging from E_0 up to E_{12} corresponding to 12 adenylylatable subunits in the GS molecule) increases under conditions of ammonium abundance (see [40,41] and references therein). From the structural point of view, bacterial GS molecules are dodecamers formed from two face-to-face hexameric rings of subunits with 12 active sites formed between the monomers [39].

Divalent cations (commonly, Mg^{2+}, Mn^{2+} or Co^{2+}) are critical for the activity of all known bacterial GSs [39–42]. According to X-ray crystallographic studies, each active center of the enzyme has two divalent cation-binding sites, n1 and n2, with the affinity of n1 for metal ions being much higher than that of n2 (both must be saturated for the GS activity to be expressed); there are also many additional metal-binding sites with relatively low affinity outside the active center of the enzyme, which are considered to be important for the conformational stability of the molecule, as well as a binding site for ammonium. A cation bound in site n1 (with a much higher affinity) is coordinated by three Glu residues (i.e. three side-chain carboxylic groups), whereas one bound in site n2 is coordinated by one His and two Glu residues (i.e. one nitrogen-donor atom of the His heterocycle and two carboxyls), and this structure is strictly conserved among different GSs [39] (note that additional nonprotein ligand(s) are one or more H_2O molecules [43]).

It has been found that the native (isolated and purified) *A. brasilense* GS shows enzymatic activity without divalent metals in the medium and therefore contains cations bound in its active centers, which is prerequisite for enzyme activity to be expressed [39,40]. However, after treating the native enzyme with 5 mM EDTA (with subsequent dialysis to remove EDTA-bound cations), a reversible loss of activity was found. Thus, while the resulting cation-free enzyme was inactive, it restored its activity after adding calculated amounts of Mg^{2+}, Mn^{2+} or Co^{2+}. The latter finding shows that the cations added are bound in the GS active centers, governed by their high affinity, so that the enzyme regains its active state. These methodological approaches [40] were useful for investigating structural changes in GS molecular conformation induced by removal or binding of activating cations as well as for probing the structural organization of the cation-binding sites in the enzyme active centers discussed below.

2.4.2 Circular Dichroism Spectroscopic Studies of the Enzyme Secondary Structure

2.4.2.1 Methodology of Circular Dichroism (CD) Spectroscopic Analysis of Protein Secondary Structure

CD spectroscopy in the UV region is one of the techniques that can be used for studying the secondary structure of proteins in solution (see [40] and references therein). The results of measurements are expressed in terms of molar ellipticity ($[\Theta]$ in deg cm^2 $dmol^{-1}$), based on a mean amino acid residue weight (MRW, assuming its average weight to be equal to 115 Da), as a function of wavelength (λ, nm) determined as $[\Theta]_\lambda = \Theta \times 100(\mathrm{MRW})/cl$, where c is the protein concentration (in mg ml^{-1}), l is the light path length (in cm) and Θ is the measured ellipticity (in degrees) at a wavelength λ. The instrument (spectropolarimeter) is calibrated with some CD standards, e.g. (+)-10-camphorsulfonic acid, having $[\Theta]_{291} = 7820$ deg cm^2 $dmol^{-1}$ or nonhygroscopic ammonium (+)-10-camphorsulfonate ($[\Theta]_{290.5} = 7910$ deg cm^2 $dmol^{-1}$).

Calculations of the content of the protein secondary structure elements are commonly performed using a standard program. It is based on fitting the experimental

spectrum to a sum of components (a negative maximum at 208 nm with molar ellipticities [Θ] around $-1.6\times10^4\,\mathrm{deg}\times\mathrm{cm}^2\times\mathrm{dmol}^{-1}$ and a shoulder at about 222 nm are typical of predominantly α-helical proteins, whereas a similarly intensive broad negative band at about 215 nm is typical of proteins rich in β-structure).

2.4.2.2 The Effect of Divalent Cations on the Secondary Structure of GS from *A. brasilense*

Comparative measurements for native partly adenylylated GS ($E_{5.3}$ corresponding to 44% of adenylylated subunits) isolated from *A. brasilense* Sp245 [44] showed that adding 1 mM Mg^{2+}, Mn^{2+} or Co^{2+} had little effect on the shape of its CD spectrum. In contrast, the CD spectrum of the native GS changed noticeably after its treatment with 5 mM EDTA and subsequent dialysis (Figure 2.6a) reflecting changes in its molecular conformation upon removal of the bound cations.

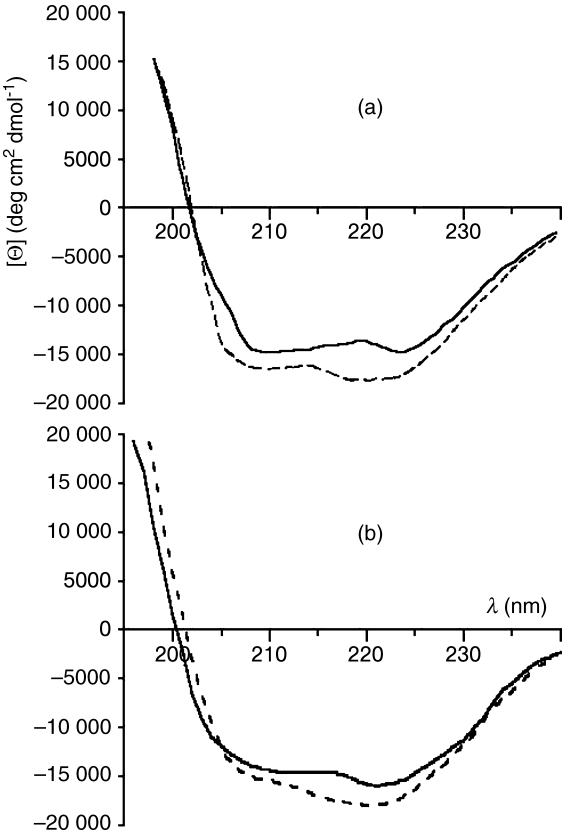

Figure 2.6 Circular dichroism spectra of native (dashed lines) and cation-free glutamine synthetase (solid lines) from *A. brasilense* Sp245: (a) partly adenylylated ($E_{5.3}$; 44% of adenylylated subunits) and unadenylylated (b) (E_0) [40,44].

Note that the general shape of the CD spectrum for the native *A. brasilense* GS was found to be somewhat different from those reported for a number of other bacterial GSs (see [40,44] and references therein). This may be connected with differences in the amino acid sequences of GSs obtained from different sources and the resulting differences in their secondary structures.

Calculations using the experimental CD spectroscopic data showed both the native and cation-free partly adenylylated enzyme ($E_{5.3}$) preparations to be highly structured (58 ± 2 and $49 \pm 3\%$ of the polypeptide as α-helices, 10 ± 2 and $20 \pm 2\%$ as β-structure, with only 32 ± 2 and $31 \pm 2\%$ unordered, respectively) [44]. Thus, the removal of cations from the native GS leads to lowering the proportion of α-helices and increasing that of the β-structure. These changes were found to be similar to those observed for native and cation-free unadenylylated (E_0) *A. brasilense* GS samples (Figure 2.6b) which had 59 ± 2 and $38 \pm 2\%$ α-helices, 13 ± 5 and $32 \pm 4\%$ β-structure, with 28 ± 3 and $30 \pm 3\%$ unordered, respectively [40].

It was found that in the case of unadenylylated GS, treatment of the native enzyme with EDTA at a lower concentration (1 mM instead of 5 mM) resulted in intermediate conformational changes ($43 \pm 1\%$ α-helices, $24 \pm 3\%$ β-structure and $32 \pm 2\%$ unordered) [40], evidently reflecting an incomplete removal of cations. On the contrary, adding divalent cations (Mg^{2+}, Mn^{2+} or Co^{2+}) to cation-free GS tended to change the enzyme conformation to one closer to the initial native preparation. Thus, *A. brasilense* GS appears to be most structured among all bacterial GSs known to date, with about 70% of its polypeptide chain being structured (α-helices + β-structural elements) in both unadenylylated and partly adenylylated enzyme. Upon removal of cations from the active centers, the proportions of the secondary structure elements change, but the protein remains similarly highly structured.

2.4.3
Emission Mössbauer Spectroscopic Analysis of the Structural Organization of the Cation-Binding Sites in the Enzyme Active Centers

2.4.3.1 Methodological Outlines and Prerequisites

The aforementioned reversible loss of the GS activity upon removal of native cations, with its restoration upon subsequent addition of a new cation, makes it possible, in principle, to replace the native cations by EMS-active $^{57}Co^{2+}$ under physiologically similar conditions [36]. In that case, active centers doped with $^{57}Co^{2+}$ ions can be probed using EMS. Nevertheless, for a correct analysis of the data to be obtained, several conditions should be observed [45]. First, when substituting the $^{57}Co^{2+}$ cation for the native cations, it is important to make sure that the metal is indeed bound within the active center; otherwise, the appearance of multiple binding sites and, consequently, many forms of cobalt would render the EMS data hardly interpretable. Second, the process of replacing the activating cations (e.g. by using natural Co^{2+} under identical conditions) should not result in an irreversible deactivation of the enzyme. In the latter case, the correspondence between the $^{57}Co^{2+}$ form in the enzyme sample under study and the cobalt(II) form in the physiologically active

enzyme would be doubtful. Finally, the quantity of the substituted $^{57}Co^{2+}$ should conform with the overall number of the cation-binding sites in the enzyme sample. It is clear that any excessive $^{57}Co^{2+}$, binding to different functional groups of the protein macromolecule beyond the active centers, can lead to an unpredictable complication of the spectra.

Fulfillment of the above-mentioned conditions is facilitated by the fact that the affinity to the cation in the enzyme active centers is usually much higher than elsewhere on the protein globule. Moreover, when the active center contains more than one binding site with different affinities to the cation and different coordination environments (as in the case with glutamine synthetase), it may be expected that using an amount of $^{57}Co^{2+}$ under the total 'saturation limit' (but higher than that necessary to saturate half the sites) would allow one to obtain information not only on the chemical forms and coordination of the cobalt but also on its distribution between the sites. The above-discussed properties of *A. brasilense* GS were found to be suitable for using the EMS technique in studying $^{57}Co^{2+}$-doped enzyme preparations [36,44,45].

2.4.3.2 Experimental Studies of *A. brasilense* GS

Measurements were performed on *A. brasilense* GS ($E_{2.2}$ corresponding to the adenylylation state 18%) using the EMS technique (according to the scheme presented in Figure 2.3). Analysis of the emission Mössbauer spectra of $^{57}Co^{2+}$-doped GS both in rapidly frozen aqueous solution and in the dry state (Figure 2.7; both spectra measured at $T = 80$ K) indeed showed in each spectrum the presence of two forms of cobalt(II) with different affinities (in view of unequal distribution of $^{57}Co^{II}$ between the forms; cf. doublets 1 and 2 in Figure 2.7) as well as with different coordination reflected by different Mössbauer parameters (Figure 2.8). The presence of the third spectral component (doublet 3 in both spectra) is related to the aftereffects of the nuclear transformation $^{57}Co \rightarrow {}^{57}Fe$ resulting in the formation of an aliovalent $^{57}Fe^{3+}$ species [34,35]. In the present case, the appearance of this component does not affect the interpretation of the data on the initial Co^{II} forms [45].

The values of isomer shifts (IS = 1.08 and 1.05–1.07 mm s^{-1} relative to α-Fe) and quadrupole splittings (QS = 3.0–3.1 and 2.3–2.4 mm s^{-1}; see Figure 2.8) obtained for doublets 1 and 2, respectively, allowed those components to be correlated with the two cation-binding sites in the GS active center (sites n2 and n1, respectively [39]). As mentioned above, these sites of bacterial GSs have different coordination environments, as well as a correspondingly lower (for site n2) and higher (for site n1) affinity to the cation. The latter difference is in line with the nonuniform distribution of $^{57}Co^{II}$ between the spectral components (as the areas of quadrupole doublets 1 and 2 in each spectrum corresponding to different $^{57}Co^{II}$ forms are significantly different; see Figure 2.7). The close (overlapping) values of the Mössbauer parameters for the corresponding $^{57}Co^{II}$ forms for GS in frozen solution and in the dry state at $T = 80$ K (see Figure 2.8) reflect the unaffected cobalt(II) microenvironment in each of the forms at the active centers in both states. This, in turn, correlates well with the conformational stability of bacterial glutamine synthetases and suggests that no significant structural changes occur upon drying the enzyme [44].

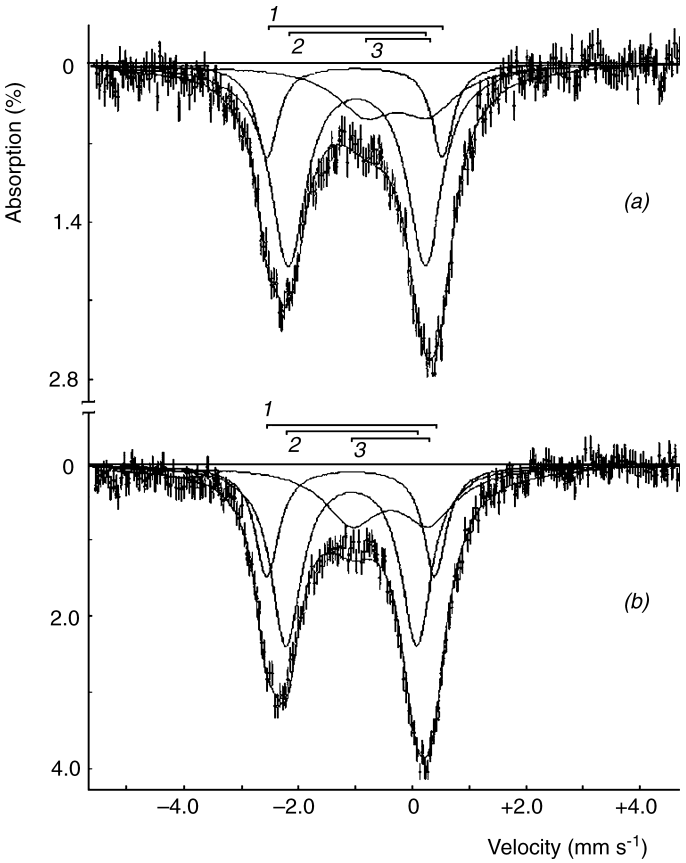

Figure 2.7 Emission Mössbauer spectra of cation-free glutamine synthetase (GS; $E_{2.2}$) from *A. brasilense* Sp245 incubated with $^{57}Co^{2+}$ for 60 min at ambient temperature (a) in rapidly frozen aqueous solution and as a dried solid (b) (measured at $T = 80$ K; intensities converted to the absorption convention). For each spectrum, the relevant subspectra (quadrupole doublets) are shown which contributed to the resulting spectrum (solid-line envelope) obtained by computer fitting to the experimental data (points with vertical error bars). The positions of the spectral components (quadrupole doublets) are indicated by horizontal square brackets above the zero lines.

The relatively low IS values for both the $^{57}Co^{II}$ forms in GS with $E_{2.2}$ (IS = 1.05 and 1.08 mm s^{-1} at $T = 80$ K; see Figure 2.8) may indicate a tetrahedral symmetry of cobalt(II) coordination. In this case, the coordination mode of all the Glu residues must be monodentate, which is often observed for cation-binding sites in metalloproteins [46] (note that there is also at least one water molecule as a ligand, according to Eads *et al.* [43]). Similarly, low IS values were found for EMS spectra of dilute frozen aqueous solutions of $^{57}Co^{II}$ complexes with amino acids (anthranilic acid and tryptophan; IS = 1.1 and 0.9 mm s^{-1}, QS = 2.7 and 2.8 mm s^{-1}, respectively), also assuming a tetrahedral symmetry [49]. Note that tetrahedral coordination (T_d) of

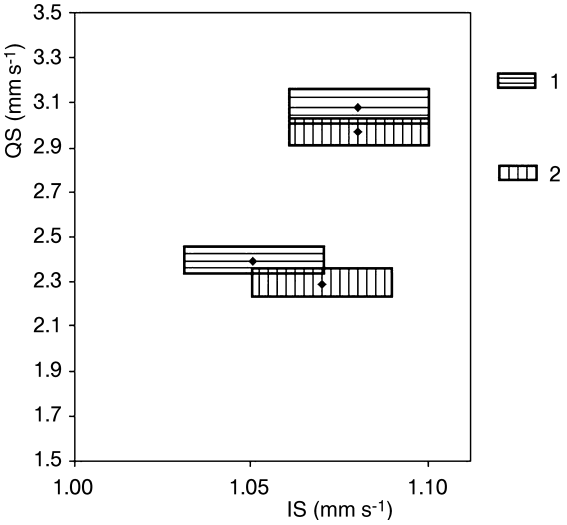

Figure 2.8 Comparison of Mössbauer parameters–isomer shift (IS, mm s^{-1}; relative to α-Fe) and quadrupole splitting (QS, mm s^{-1}) – for different forms of [^{57}Co]-cobalt(II) in $^{57}Co^{II}$-doped glutamine synthetase from *A. brasilense* Sp245 (1) in rapidly frozen aqueous solution and in the solid (dried) state (2) (measured at $T = 80$ K).

cobalt(II) is possible [46–48], although in many proteins cobalt was found to have preference for higher coordination numbers, i.e. 5 and 6 (see [47] and references cited therein).

2.4.3.3 **Conclusions and Outlook**

The EMS technique, recently applied for the first time to probing cation binding in the active centers of a bacterial enzyme doped with the radioactive ^{57}Co isotope [36,44], has shown that each active center of glutamine synthetase from azospirilla has two cation-binding sites with different affinities to cobalt(II) as an activating cation and with different coordination symmetry. The results obtained are in good agreement with the current literature data on the structural organization of the active centers in bacterial adenylylatable glutamine synthetases [39,41].

For future structural investigations of the active centers in metal-containing biocomplexes and enzymes, the advantages of using the highly sensitive and selective emission variant of Mössbauer spectroscopy can hardly be overestimated. This nuclear chemistry technique has recently been shown to be sensitive also (i) to the effects of competitive binding of different activating cations ($Mn^{2+} + {}^{57}Co^{2+}$, with a redistribution of the latter between the two sites in GS) at the active centers, showing that heterobinuclear two-metal-ion catalysis by GS is principally possible, as well as (ii) to fine structural changes induced by covalent modifications of the enzyme molecule related to its activity [50]. The results obtained are highly promising for

further study of the molecular mechanisms of enzymatic activity regulation and enzyme–substrate biospecific interactions using the unique possibilities of the EMS technique.

Besides cobalt-activated enzymes, EMS may be applicable to studying other metalloproteins upon substituting ^{57}Co for the native metal. For instance, substitution of Co^{2+} (as an optically active probe) for Zn^{2+} has been used extensively in optical spectroscopic methods to obtain structural information on zinc metalloproteins and is based on the fact that these two cations typically exhibit similar coordination geometries for a given ligand set [48]. Thus, the possibility of using ^{57}Co as a substituting probe, considering also the exceptionally high sensitivity of the EMS technique, can significantly expand the limits of its applicability in biochemistry and related fields in the life sciences.

2.5 General Conclusions and Future Directions of Research

The highly sophisticated field of bioscience comprising the interactions of microorganisms with their hosts (higher organisms) has been increasingly attracting attention during the past decade both in basic research and in applied fields, particularly those related to agricultural and environmental biotechnology. As for plant–microbe interactions, the subject can be reasonably classified and accordingly divided into a few major categories [51]: (i) the physiological and biochemical properties and responses of the macropartner (the host plant), (ii) the corresponding properties and behavior of the micropartner (consortia of plant-associated microorganisms, in particular, in the rhizosphere), as well as (iii) any processes or phenomena directly related to their interactions per se, including remote exchange of molecular signals and their perception, microbial quorum sensing and its inhibition (including chemical and enzymatic 'quorum quenching' or 'anti-quorum sensing', contact and intercellular interactions, the effects and role of the chemical composition and conditions of the medium, and so on (see [51] and references cited therein).

It is clear that any purely chemical (i.e. abiotic) processes, induced in the rhizosphere by the presence or formation of chemically active species (e.g. metal ions, oxidizing agents, etc.), which result in chemical depletion, inactivation or degradation of any biomolecules directly involved in plant–microbe interactions via their binding and/or redox transformation, would inevitably affect these biologically specific interactions. However, in the rapidly increasing pool of basic and applied research data related to plant–microbe interactions (see, e.g. the recent highly informative review [25]), such chemical interferences seem to have been paid significantly less attention so far than they really deserve [13,51,52] considering their possible contribution to the overall effects. This imbalance in approaching the whole problem, leading to a virtual imbalance in understanding the diversity of molecular mechanisms underlying the processes and phenomena in highly sophisticated soil–plant–microbe systems, still remains to be corrected by increasingly involving

experts from chemical and physical sciences and applying a complex of relevant modern instrumental techniques.

In order to illustrate the applicability of a range of instrumental techniques in bioscience, a number of recent stimulating reviews and highly informative experimental reports may be recommended, such as: applications of vibrational spectroscopy in microbiology [6,8–10,53]; noninvasive characterization of microbial cultures and various metabolic transformations using multielement NMR spectroscopy [54]; X-ray crystallography in studying biological complexes [55]; biological, agricultural and environmental research using X-ray microscopy and microradiography [56] and X-ray absorption spectroscopy [57]; surface characterization of bacteria using X-ray photoelectron spectroscopy (XPS), time-of-flight secondary-ion mass spectrometry (ToF-SIMS) [58] and atomic force microscopy (AFM) [59]; inductively coupled plasma–mass spectrometry (ICP-MS) as a multielement and multiisotope highly sensitive analytical tool [60]; novel biochemical [33] and microbiological applications of the emission variant of Mössbauer (nuclear γ-resonance) spectroscopy (based on the use of ^{57}Co) [10] as well as its traditionally used transmission variant using the stable ^{57}Fe isotope [31,32], its combination with electron paramagnetic resonance (EPR) spectroscopy [61]; stable isotope technologies in studying plant–microbe interactions [62], and so on.

Acknowledgments

The author is grateful to many of his colleagues both at the Institute in Saratov and from other research organizations, who have contributed to the studies considered in this chapter, for their help in experimental work, long-term collaboration and many stimulating discussions. Support for the author's research in Russia and for his international collaboration, which contributed in part to the interdisciplinary fields considered in this chapter, has been provided within the recent years by grants from INTAS (EC, Brussels, Belgium; Project 96-1015), NATO (Projects LST. CLG.977664, LST.EV.980141, LST.NR.CLG.981092, CBP.NR.NREV.981748, ESP. NR.NRCLG 982857), the Russian Academy of Sciences' Commission (Grant No. 205 under the 6th Competition-Expertise of research projects) as well as under the Agreements on Scientific Cooperation between the Russian and Hungarian Academies of Sciences for 2002–2004 and 2005–2007.

References

1 Ivanov, V.T. and Gottikh, B.P. (1999) *Herald of the Russian Academy of Sciences*, **69**, 208–214.

2 Bashan, Y., Holguin, G. and de-Bashan, L.E. (2004) *Canadian Journal of Microbiology*, **50**, 521–577.

3 Naumann, D., Keller, S., Helm, D., Schultz, Ch. and Schrader, B. (1995) *Journal of Molecular Structure*, **347**, 399–405.

4 Schmitt, J. and Flemming, H.-C. (1998) *International Biodeterioration & Biodegradation*, **41**, 1–11.

5 Schrader, B., Dippel, B., Erb, I., Keller, S., Löchte, T., Schulz, H., Tatsch, E. and Wessel, S. (1999) *Journal of Molecular Structure*, **480–481**, 21–32.

6 Naumann, D. (2000) Infrared spectroscopy in microbiology, in: *Encyclopedia of Analytical Chemistry* (ed. R. A. Meyers), John Wiley & Sons, Ltd, Chichester, UK, pp. 102–131.

7 Kamnev, A.A., Tarantilis, P.A., Antonyuk, L.P., Bespalova, L.A., Polissiou, M.G., Colina, M., Gardiner, P.H.E. and Ignatov, V.V. (2001) *Journal of Molecular Structure*, **563–564**, 199–207.

8 Jiang, W., Saxena, A., Song, B., Ward, B.B., Beveridge, T.J. and Myneni, S.C.B. (2004) *Langmuir*, **20**, 11433–11442.

9 Yu, C. and Irudayaraj, J. (2005) *Biopolymers*, **77**, 368–377.

10 Kamnev, A.A., Tugarova, A.V., Antonyuk, L.P., Tarantilis, P.A., Kulikov, L.A., Perfiliev, Yu.D., Polissiou, M.G. and Gardiner, P.H.E. (2006) *Analytica Chimica Acta*, **573–574**, 445–452.

11 Belimov, A.A., Kunakova, A.M., Safronova, V.I., Stepanok, V.V., Yudkin, L.Yu., Alekseev, Yu.V. and Kozhemyakov, A.V. (2004) *Microbiology (Moscow)*, **73**, 99–106.

12 Tugarova, A.V., Kamnev, A.A., Antonyuk, L.P. and Gardiner, P.H.E. (2006) *Azospirillum brasilense* resistance to some heavy metals, in: *Metal Ions in Biology and Medicine*, vol. 9 (eds M.C. Alpoim, P.V. Morais, M.A. Santos, A.J. Cristóvão, J.A. Centeno and Ph. Collery), John Libbey Eurotext, Paris, pp. 242–245.

13 Kamnev, A.A. and van der Lelie, D. (2000) *Bioscience Reports*, **20**, 239–258.

14 Glick, B.R. (2003) *Biotechnology Advances*, **21**, 383–393.

15 Khan, A.G. (2005) *Journal of Trace Elements in Medicine and Biology*, **18**, 355–364.

16 Biró, B., Köves-Péchy, K., Tsimilli-Michael, M. and Strasser, R.J. (2006) Role of the beneficial microsymbionts in the plant performance and plant fitness, in: *Soil Biology, vol. 7: Microbial Activity in the Rhizosphere* (eds K.G. Mukerji, C. Manoharachary and J. Singh), Springer, Berlin, Heidelberg, pp. 265–296.

17 Lyubun, Ye.V., Fritzsche, A., Chernyshova, M.P., Dudel, E.G. and Fedorov, E.E. (2006) *Plant and Soil*, **286**, 219–227.

18 Kamnev, A.A., Renou-Gonnord, M.-F., Antonyuk, L.P., Colina, M., Chernyshev, A.V., Frolov, I. and Ignatov, V.V. (1997) *Biochemistry and Molecular Biology International*, **41**, 123–130.

19 Kamnev, A.A., Ristić, M., Antonyuk, L.P., Chernyshev, A.V. and Ignatov, V.V. (1997) *Journal of Molecular Structure*, *408/409*, pp. 201–205.

20 Kamnev, A.A., Antonyuk, L.P., Matora, L.Yu., Serebrennikova, O.B., Sumaroka, M.V., Colina, M., Renou-Gonnord, M.-F. and Ignatov, V.V. (1999) *Journal of Molecular Structure*, **480–481**, 387–393.

21 Ignatov, O.V., Kamnev, A.A., Markina, L.N., Antonyuk, L.P., Colina, M. and Ignatov, V.V. (2001) *Applied Biochemistry and Microbiology (Moscow)*, **37**, 219–223.

22 Kadouri, D., Jurkevitch, E. and Okon, Y. (2003) *Applied and Environmental Microbiology*, **69**, 3244–3250.

23 Kadouri, D., Jurkevitch, E., Okon, Y. and Castro-Sowinski, S. (2005) *Critical Reviews in Microbiology*, **31**, 55–67.

24 Kamnev, A.A., Antonyuk, L.P., Tugarova, A.V., Tarantilis, P.A., Polissiou, M.G. and Gardiner, P.H.E. (2002) *Journal of Molecular Structure*, **610**, 127–131.

25 Somers, E., Vanderleyden, J. and Srinivasan, M. (2004) *Critical Reviews in Microbiology*, **30**, 205–240.

26 Olubai, O., Caudales, R., Atkinson, A. and Neyra, C.A. (1998) *Canadian Journal of Microbiology*, **44**, 386–390.

27 Kirchhof, G., Schloter, M., Aßmus, B. and Hartmann, A. (1997) *Soil Biology & Biochemistry*, **29**, 853–862.

28 Rothballer, M., Schmid, M. and Hartmann, A. (2003) *Symbiosis*, **34**, 261–279.

29 Lodewyckx, C., Vangronsveld, J., Porteous, F., Moore, E.R.B., Taghavi, S. and van der

Lelie, D. (2002) *Critical Reviews in Plant Sciences*, **21**, 583–606.

30 Kamnev, A.A., Tugarova, A.V., Antonyuk, L.P., Tarantilis, P.A., Polissiou, M.G. and Gardiner, P.H.E. (2005) *Journal of Trace Elements in Medicine and Biology*, **19**, 91–95.

31 Oshtrakh, M.I. (2004) *Spectrochimica Acta A*, **60**, 217–234.

32 Krebs, C., Price, J.C., Baldwin, J., Saleh, L., Green, M.T. and Bollinger, J.M. Jr (2005) *Inorganic Chemistry*, **44**, 742–757.

33 Kamnev, A.A. (2005) *Journal of Molecular Structure*, **744–747**, 161–167.

34 Vértes, A. and Nagy, D.L. (eds) (1990) *Mössbauer Spectroscopy of Frozen Solutions*. Akad. Kiadó, Budapest, 1990, Chapter 6 (Russian edition) (1998) (ed. Yu.D. Perfiliev), Mir, Moscow, pp. 271–293.

35 Perfiliev, Yu.D., Rusakov, V.S., Kulikov, L.A., Kamnev, A.A. and Alkhatib, K. (2006) *Hyperfine Interactions*, **167**, 881–885.

36 Kamnev, A.A., Antonyuk, L.P., Smirnova, V.E., Serebrennikova, O.B., Kulikov, L.A. and Perfiliev, Yu.D. (2002) *Analytical and Bioanalytical Chemistry*, **372**, 431–435.

37 Kamnev, A.A., Antonyuk, L.P., Kulikov, L.A. and Perfiliev, Yu.D. (2004) *BioMetals*, **17**, 457–466.

38 Lloyd, J.R. (2003) *FEMS Microbiology Reviews*, **27**, 411–425.

39 Eisenberg, D., Gill, H.S., Pfluegl, G.M.U. and Rotstein, S.H. (2000) *Biochimica et Biophysica Acta*, **1477**, 122–145.

40 Antonyuk, L.P., Smirnova, V.E., Kamnev, A.A., Serebrennikova, O.B., Vanoni, M.A., Zanetti, G., Kudelina, I.A., Sokolov, O.I. and Ignatov, V.V. (2001) *BioMetals*, **14**, 13–22.

41 Antonyuk, L.P. (2007) *Applied Biochemistry and Microbiology (Moscow)*, **43**, 244–249.

42 Bespalova, L.A., Antonyuk, L.P. and Ignatov, V.V. (1999) *BioMetals*, **12**, 115–121.

43 Eads, C.D., LoBrutto, R., Kumar, A. and Villafranca, J.J. (1988) *Biochemistry*, **27**, 165–170.

44 Kamnev, A.A., Antonyuk, L.P., Smirnova, V.E., Kulikov, L.A., Perfiliev, Yu.D., Kudelina, I.A., Kuzmann, E. and Vértes, A. (2004) *Biopolymers*, **74**, 64–68.

45 Kamnev, A.A., Antonyuk, L.P., Kulikov, L.A., Perfiliev, Yu.D., Kuzmann, E. and Vértes, A. (2005) *Bulletin of the Russian Academy of Sciences (Physics)*, **69**, 1561–1565.

46 Holm, R.H., Kennepohl, P. and Solomon, E.I. (1996) *Chemical Reviews*, **96**, 2239–2314.

47 Innocenti, A., Zimmerman, S., Ferry, J.G., Scozzafava, A. and Supuran, C.T. (2004) *Bioorganic & Medicinal Chemistry Letters*, **14**, 3327–3331.

48 Namuswe, F. and Goldberg, D.P. (2006) *Chemical Communications*, (22), 2326–2328.

49 Kamnev, A.A., Kulikov, L.A., Perfiliev, Yu.D., Antonyuk, L.P., Kuzmann, E. and Vértes, A. (2005) *Hyperfine Interactions*, **165**, 303–308.

50 Kamnev, A.A., Antonyuk, L.P., Smirnova, V.E., Kulikov, L.A., Perfiliev, Yu.D., Kuzmann, E. and Vértes, A. (2005) *FEBS Journal*, **272** (Suppl 1), 10.

51 Kamnev, A.A. (2008) Metals in soil *versus* plant-microbe interactions: biotic and chemical interferences, in: *Plant-Microbe Interaction* (eds E.A. Barka and Ch. Clément), Research Signpost, Trivandrum (Kerala, India), Chapter 13, pp. 291–318.

52 Kamnev, A.A. (2003) Phytoremediation of heavy metals: an overview, in: *Recent Advances in Marine Biotechnology, vol. 8: Bioremediation* (eds M. Fingerman and R. Nagabhushanam), Science Publishers, Inc., Enfield, NH, USA, pp. 269–317.

53 Aroca, R. (2006) *Surface-Enhanced Vibrational Spectroscopy*, John Wiley & Sons, Ltd, Chichester, 400 pp.

54 Lens, P.N.L. and Hemminga, M.A. (1998) *Biodegradation*, **9**, 393–409.

55 Sommerhalter, M., Lieberman, R.L. and Rosenzweig, A.C. (2005) *Inorganic Chemistry*, **44**, 770–778.

56 Reale, L., Lai, A., Bellucci, I., Faenov, A., Pikuz, T., Flora, F., Spanò, L., Poma, A.,

Limongi, T., Palladino, L., Ritucci, A., Tomassetti, G., Petrocelli, G. and Martellucci, S. (2006) *Microscopy Research and Technique*, **69**, 666–674.

57 Prange, A. and Modrow, H. (2002) *Reviews in Environmental Science and Biotechnology*, **1**, 259–276.

58 Pradier, C.M., Rubio, C., Poleunis, C., Bertrand, P., Marcus, P. and Compère, C. (2005) *Journal of Physical Chemistry B*, **109**, 9540–9549.

59 Teschke, O. (2005) *Microscopy Research and Technique*, **67**, 312–316.

60 Cottingham, K. (2004) *Analytical Chemistry*, **76**, 35A–38A.

61 Schünemann, V., Jung, C., Lendzian, F., Barra, A.-L., Teschner, T. and Trautwein, A.X. (2004) *Hyperfine Interactions*, **156/157**, 247–256.

62 Prosser, J.I., Rangel-Castro, J.I. and Killham, K. (2006) *Current Opinion in Biotechnology*, **17**, 98–102.